This article was downloaded by:
On: *14 January 2011*
Access details: *Access Details: Free Access*
Publisher *Taylor & Francis*
Informa Ltd Registered in England and Wales Registered Number: 1072954 Registered office: Mortimer House, 37-41 Mortimer Street, London W1T 3JH, UK

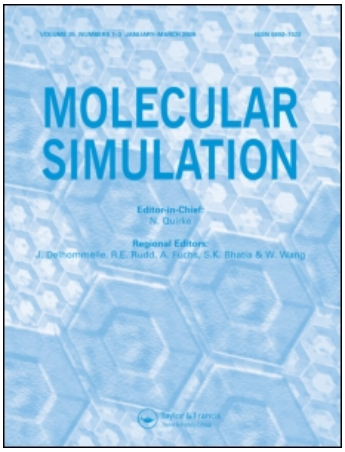

Molecular Simulation
Publication details, including instructions for authors and subscription information:
http://www.informaworld.com/smpp/title~content=t713644482

Analysis of agonism by dopamine at the dopaminergic D 2 G-protein coupled receptor based on comparative modelling of rhodopsin

Benjamin G. Tehan[a]; Edward J. Lloyd[a]; Margaret G. Wong[b]; David K. Chalmers[a]
[a] Department of Medicinal Chemistry, Victorian College of Pharmacy, Monash University, Parkville, Australia [b] Department of Applied Chemistry, Swinburne University of Technology, Hawthorn, Australia

Online publication date: 26 October 2010

To cite this Article Tehan, Benjamin G. , Lloyd, Edward J. , Wong, Margaret G. and Chalmers, David K.(2002) 'Analysis of agonism by dopamine at the dopaminergic D 2 G-protein coupled receptor based on comparative modelling of rhodopsin', Molecular Simulation, 28: 10, 865 — 888
To link to this Article: DOI: 10.1080/0892702021000002548
URL: http://dx.doi.org/10.1080/0892702021000002548

PLEASE SCROLL DOWN FOR ARTICLE

Full terms and conditions of use: http://www.informaworld.com/terms-and-conditions-of-access.pdf

This article may be used for research, teaching and private study purposes. Any substantial or systematic reproduction, re-distribution, re-selling, loan or sub-licensing, systematic supply or distribution in any form to anyone is expressly forbidden.

The publisher does not give any warranty express or implied or make any representation that the contents will be complete or accurate or up to date. The accuracy of any instructions, formulae and drug doses should be independently verified with primary sources. The publisher shall not be liable for any loss, actions, claims, proceedings, demand or costs or damages whatsoever or howsoever caused arising directly or indirectly in connection with or arising out of the use of this material.

Molecular Simulation, 2002 Vol. 28 (10–11), pp. 865–888

Taylor & Francis
Taylor & Francis Group

Downloaded At: 18:41 14 January 2011

ANALYSIS OF AGONISM BY DOPAMINE AT THE DOPAMINERGIC D_2 G-PROTEIN COUPLED RECEPTOR BASED ON COMPARATIVE MODELLING OF RHODOPSIN

BENJAMIN G. TEHAN[a], EDWARD J. LLOYD[a], MARGARET G. WONG[b] and DAVID K. CHALMERS[a,*]

[a]*Department of Medicinal Chemistry, Victorian College of Pharmacy, Monash University, 381 Royal Parade, Parkville 3052, Australia;* [b]*Department of Applied Chemistry, Swinburne University of Technology, John Street, Hawthorn 3122, Australia*

(Received March 2001; In final form November 2001)

A number of theoretical dopaminergic D_2 models were constructed using comparative modelling techniques. The models constructed were based on the recently published crystal structure of rhodopsin. D_2 models were constructed without any ligands bound in the active site and also with the endogenous agonist, dopamine, bound in the active site. Comparison of the bound and unbound models revealed the importance of the chi angle of serine 197 and the effect this has on the bending of helix 5 when an agonist is present in the binding site.

Keywords: Dopamine, D_2; G-protein coupled receptor; Rhodopsin; Agonists; Activation

INTRODUCTION

The superfamily of G-protein coupled receptors (GPCRs) constitutes the largest and most diverse group of transmembrane proteins involved in signal transduction. They are activated by a wide range of extracellular ligands

*Corresponding author.

ISSN 0892-7022 © 2002 Taylor & Francis Ltd
DOI: 10.1080/0892702021000002548

Downloaded At: 18:41 14 January 2011

including small biogenic amines, large protein hormones, neuropeptides and chemokines. GPCRs are also fundamental receptors for the sensory perception of light, taste and smell. They all share one similar characteristic, the seven distinct hydrophobic regions, each of these 20–30 amino acids in length within their sequence [1]. These hydrophobic regions form the seven transmembrane domains of these receptors, hence the alternative name for this family, 7TM receptors.

GPCRs represent one of the most important families of drug targets for the pharmaceutical industry. A survey done in 1995 by Glaxo Wellcome states that of the top 100 best selling prescription drugs, more than 20% exert their therapeutic effect by targeting GPCRs [2], whilst over 50% of all modern drugs are targeted at GPCRs [3].

GPCRs represent one of the primary mechanisms by which cells sense and respond to their external environment. The information from an extracellularly occurring receptor-ligand recognition event is transferred through conformational rearrangements within the transmembrane portion of the receptor protein to the intracellular compartment. The ligand induced activation of the receptor, in conjunction with heterotrimeric G-proteins, leads to a multistep cascade of signal transduction events. This multistep cascade involves intracellular effectors and subsequent generation of second messengers that are specific to the ligand type and the distinct member of the GPCR family involved in the process. This all eventually leads to the physiological response of the cell to the stimulus. The enormous diversity of receptors, G-proteins and effectors, together with the widespread distribution of receptors across many tissues, reflects the important role that this superfamily plays in regulating physiological and pathophysiological processes.

Schizophrenia is a physiological condition resulting from a chemical imbalance within the brain. The dopamine D_2 G protein-coupled receptor has been associated with psychosis and the positive symptomatology of schizophrenia. It has been proposed that several psychiatric illnesses are caused by hyperdopaminergic activity in dopaminergic pathways. The hypothesis that the dopaminergic system is overactive in schizophrenia is based on the finding of a correlation between the potency of neuroleptics as dopamine antagonists and their clinically effective doses [4]. Therefore, in an effort to gain a greater understanding of the D_2 GPCR and the residues involved in the conformational rearrangement within the transmembrane region, a number of theoretical models were constructed. The models constructed were based on the recently published crystal structure of rhodopsin [5]. D_2 models were constructed without any ligands bound in the active site and also with the endogenous agonist, dopamine, bound in the active site.

Downloaded At: 18:41 14 January 2011

METHOD

Method Overview

Six dopamine D_2 receptor models, three with dopamine bound in the active site and three without, were constructed by initially creating an alignment of D_2 onto rhodopsin. This was done by creating a Threader database file from the recently published rhodopsin crystal structure [5] (1F88.pdb) [6], by running Procheck [7,8], naccess [9] and strsum [10] on the structure. threader [10] in conjunction with the database file created was then used to align the sequence of D_2 onto the sequence of rhodopsin giving an alignment file. The alignment file was then examined within Seaview [11] and altered so as to align highly conserved residues within all GPCR's according to Trump–Kallmeyer [12] and other important characteristics, such as disulfide bonds [5].

The next step was the three-dimensional D_2 model generation. Modeller [13] was used and was run on the alignment files to create tertiary structures of the D_2 receptor. Additional constraints were placed upon the alignment files according to various mutagenesis [14] and modelling studies [15]. The resulting structures were then minimised within Sybyl 6.7 [16] using Kollman all-atom charges and force field [17]. The models created were analysed within Sybyl to check their compliance with mutagenesis and substituted cysteine accessibility method (SCAM) studies [14,18–24] as well as a number of other factors. The numbering scheme of the constructed receptors was based on the dopamine D_2 long (P14416) sequence from Swiss-Prot [25].

Generating the Alignment of D_2 onto Rhodopsin

Construction of the Threader Database File

The threader database file created contains a numerical representation of the rhodopsin crystal structure it was derived from. This gives an indication as to the type, volume and characteristics of the residue within the sequence of the protein. This information is crucial for the threading of the D_2 sequence onto that of rhodopsin. However, before this can be done, the rhodopsin structure must be analysed, and altered if necessary, and then a number of files must be created within Procheck.

Procheck checks the stereochemical quality of a protein structure, producing a number of postscript plots analysing its overall and residue-by-residue geometry. It also produces two files needed to create a threader database file. One file holds the "cleaned-up" version of the original PDB file, with any wrong atom-labels

Downloaded At: 18:41 14 January 2011

corrected in accordance with the IUPAC naming conventions. The other file contains residue information used by the phi/psi plotting programs. Procheck also produces a number of log files that give an indication as to which residues are causing problems in construction of the database file. Chain breaks within the crystal structure of rhodopsin were identified from the Procheck log files and manually fixed within Sybyl. The added residues and a 6 Å radius around the residues added were then minimised for 100 iterations, so as to only make small local structural alterations, with Kollman all atom charges, and the Kollman force field. A number of other incorrect residues were identified and fixed. This final structure was then run through Procheck again to check for compliance of the psi/phi angles of all residues altered. If disallowed psi/phi angles were found the residues implicated were then manually altered within Sybyl and the minimisation process was repeated until all added residues complied with Procheck allowed regions. The resulting rhodopsin structure (lF88_complete.pdb) was then compared to the original structure 1F88.pdb, by comparing an all atom alignment and a Cα carbon alignment.

Naccess, a stand alone program that calculates the atomic accessible surface defined by rolling a probe of given size around a van der Waals surface, was then run to create a residue accessibility file. The residue accessibility file contains summed atomic accessible surface areas over each protein or nucleic acid residue. This file is necessary for creating a threader database file.

Strsum, which is short for structure summariser, is used to generate the TDB (Threader database) files so that users can include their own structures in the threader fold library. Strsum combines the three output files to generate the threader database file.

The resulting tdb file is then placed into the fold library directory and threader is ready to be run on the threader database file created.

Running Threader

Threader was run with the depth flag set to 1000 to obtain the best result. The print alignment in modeller format was set to obtain an output for putting into Modeller. The sequence similarity (−S flag) was adjusted, to 100, so the alignment of the sequences was not based purely on threading, giving a 50–50 mixture of threading and sequence alignment.

The modeller alignment file created in threader is checked within Seaview [11] to see if there is a good correlation between positive, negative, hydrophobic and hydrophilic residues for the two sequences.

The alignment is then ready for input into Modeller.

Downloaded At: 18:41 14 January 2011

Three-dimensional D_2 Model Generation

Modeller calculates a three-dimensional full-atom model, from an alignment of two sequences and one corresponding known structure. Modeller does this by satisfying specific spatial restraints [26]. In this case, the restraints are derived from the rhodopsin crystal structure and a database of protein structure alignments [27], the three-dimensional structure created is that of dopamine D_2. This overall process is termed comparative modelling.

MODELLER requires an alignment file, a restraints file and an input file in order to run, as well as the pdb structure that the model is to be based on. The alignment file obtained from threader must be further altered to include breaks within the sequence alignments. The restraints file contains constraints added to the model construction according to mutagenesis and modelling studies. The input file contains pointers to the restraints file, alignment file, the pdb structure onto which the model is based, various subroutines to be called and additional data such as the number of models to be constructed. The resulting output files of modeller that are of interest are in pdb format.

Analysing the pdb Files from Modeller

The resultant pdb files from modeller need to be modified before minimisation takes place, as they are created with a number of missing disulfide bonds and breaks within their chains. There were also a number of incorrect atom types created that were altered so as to comply with the Kollman All Atom force field. Minimisation of the joins and disulfide linkages was done by selecting the residues of interest and a 6 Å radius around the residues and minimising for only 100 iterations, so as to only make small local structural alterations, with Kollman all atom charges, and the Kollman force field. A number of different sequential methods of minimisation were employed to check for consistency in results; for example, joins were minimised in their numeric sequential order and joins were minimised according to their relative arrangement to one another.

Minimising the Potential Energy of the Protein

The pdb files were minimised in three steps in order to obtain a structure that was as refined as possible, without having to undergo molecular dynamics and possibly lose the similarity to rhodopsin:

1. minimise only hydrogens, holding the rest of molecule in aggregate,

2. minimise only sidechains, holding the backbone in aggregate,
3. minimise the whole molecule.

Each minimisation step was for 10,000 iterations or until a RMS gradient of 0.01 kcal/mol was reached using Kollman all atom charges and Kollman force field.

Downloaded At: 18:41 14 January 2011

Analysing the Bound and Unbound Receptor States

The three resulting pdb files without the agonist dopamine were then compared to one another and the three resulting pdb files with the agonist dopamine were also compared to one another. This was done using the following criteria:

- The RMS fit for all atoms and for Cα carbons was calculated for the differing groups. This was done using "fit monomer" and by selecting all residues that were aligned onto the rhodopsin crystal structure, as the residues of interest.
- The calculated energies (kcal/mol) of the two groups of three structures using differing Force Fields and Kollman Charges was performed.
- The Procheck phi/psi region plot statistics of residues of the two groups were compared along with the rhodopsin structure these were based upon.
- The pdb files were also visualised to see if they all complied with SCAM data from a number of papers [14,18–24].
- Models had their secondary structure predicted, by "assign secondary structure" within Sybyl, and this was compared to theoretical predictions.

Comparing the Bound and Unbound Receptor States

The two resulting receptor states were then compared to one another using the following criteria.

- Resulting structures were aligned on one another using "fit monomer" of all the residues that were aligned to residues from the crystal structure of rhodopsin.
- Particular interest was paid to residues that had the greatest RMS fit deviation and were within the proposed binding site.
- Residues and hydrogen bonds around the active site were examined in detail.
- Helices thought to be involved in conformational rearrangement were examined relative to the state of unbound receptor helices.

Downloaded At: 18:41 14 January 2011

RESULTS AND DISCUSSION

Generating the Alignment of D_2 onto Rhodopsin

Construction of the Threader Database File

Analyses of the crystal structure of rhodopsin revealed two chain breaks between

1. A235 and S240, missing residues QQQE.
2. P327 and S334, missing residues LGDDEA.

Break 1 is located eight residues after H5 in the cytoplasmic loop C3. The complete C3 loop although not included in the original model is said not to fold over the helical region. Break 2 is located four residues after the cysteine linkages at the end of helix loop H8. This missing section is said to cover H8 from the solvent region [5].

This was taken into consideration when remodelling these sections of the protein.

Additional to the two chain breaks present in the crystal structure, there were a number of incorrect residues present in the structure.

T335 was missing the sidechain of this residue and S334 was missing the hydroxy group off its sidechain. These were added according to allowed chi angles of the sidechain and steric constraints of the protein.

The resulting structure was then minimised according to the method set out in "Construction of the threader database file" section.

The RMS fit of the modified and original rhodopsin models, see Table I, show an extremely close match over the 333 residues that the structures had in common, the main discrepancies occurring near the chain breaks where the additional residues were placed.

Running Threader

The results from threader although not definitive were of interest, because threader was concurrently run on two crystal structures of bacteriorhodopsin [28]

TABLE I Modified structure of rhodopsin compared to the original crystal structure

	RMS fit (Å^2) of Cα carbons	*RMS fit (Å^2) of whole carbons*
Modified structure	0.0975	0.1580

Downloaded At: 18:41 14 January 2011

TABLE II Statistical output from Threader

Pairwise energy	*Z-score (native) core-shuffled*	*Z-score (mean) core-shuffled*	*Z-score (minimum) core-shuffled*	*Z-score (mean) pairwise-energy*	*Z-score (weighted) pairwise-energy*	*Percentage of structure aligned*	*Percentage of sequence aligned*	*Threader pdb code*
−490.7354	−0.84	2.72	0.64	0.86	0.87	85.9	67.5	1f8800
−492.1607	−1.08	3.13	0.03	0.86	0.87	84.8	66.6	1f88A0
−342.7945	−4.36	2.33	−0.16	−9.99	−9.99	97.8	50.1	1f4zA0
−34.5434	−5.06	2.08	−0.25	−9.99	−9.99	96.5	49.4	1f50A0

Only 9 of the 17 columns are shown.

Downloaded At: 18:41 14 January 2011

determined by X-ray diffraction at differing resolutions. This was done as a comparison against the recently determined rhodopsin model.

Usually, when analysing the statistical output from threader the weighted pairwise energy *Z*-score is used as the primary field for selecting a correct match, and a value greater than 2 would indicate a possible match. However, when using a small library of folds, as in this case, the *Z*-scores from pairwise energy may not be a useful measure of significance and checking the core-shuffled *Z*-scores is advised.

Both the mean and minimum core-shuffled *Z*-scores state that a large positive value indicates a correct match and a negative value indicates probably an incorrect match. The native core-shuffled *Z*-score denotes how low the model energy is in comparison to the native energy of the template structure; here a value greater than one indicates a probably incorrect match. From analysis of the core-shuffled *Z*-scores obtained, see Table II, we can say that IF88 is a better match than that of IF4Z and 1F50, and the latter two may be incorrect matches. IF88A0 is the threader database file created from the unmodified version of the crystal structure, whereas 1F8800 is the threader database file created in the procedure outlined in 'Construction of the threader database file" section. Both of the 1F88 matches are of approximately equal significance.

Analysing the Alignment File

The original alignment file is checked within Seaview to see if there is a good correlation between positive, negative, hydrophobic and hydrophilic residues for the two sequences.

Highly conserved residues within each helix were adjusted so as to ensure their alignment if they were not aligned already.

- TM4 had to be shifted two residues so as to align the highly conserved tryptophan ($W160_{D2}$).
- TM6 had to be shifted one residue so as to align the highly conserved tryptophan ($W386_{D2}$) and proline ($P388_{D2}$) residues.

Also, importantly, the cysteine (C l82$_{D2}$) residue had to be adjusted to correspond with the ($C187_{RHO}$) that is involved in the disulfide linkage with the highly conserved TM3 cysteine ($C110_{RHO}$/$C107_{D2}$). This was very important as this linkage constrains the second extracellular (EII) loop of both rhodopsin and D_2. In the crystal structure of rhodopsin, this loop folds deeply into the centre of rhodopsin and places this 1oop in contact with retinal. This is thought to be the

case for D_2 and most other GPCRs, with this loop also being implicated as being in proximity with binding site [5].

The resultant alignment, see Fig. 1, shown in single amino acid nomenclature shows a high degree of hydrophobicity in the transmembrane regions, as would be expected for a membrane bound receptors.

Downloaded At: 18:41 14 January 2011

Three-dimensional D_2 Model Generation

Adjusting the Alignment File

The adjusted alignment file from threader must be further altered to include breaks within the sequence alignments, where no alignment takes place.

In the alignment file construction 100 non-aligned residues between helices 5 and 6 were removed. This was because Modeller is unable to deal with more than 100 non-aligned residues.

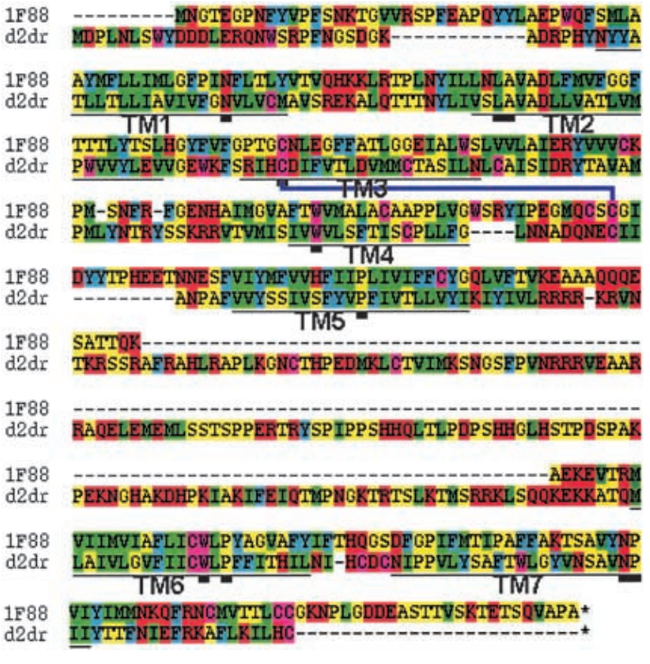

FIGURE 1 Final alignment of dopamine D_2 with rhodopsin 1F88. The highly conserved residues used in the alignment of the sequences are shown with a small black box beneath them. The highly conserved disulfide linkage in extracellular loop EII is shown by a line connecting the corresponding cysteines. The transmembrane regions are shown sequentially with a thin black line below them. Gaps within the sequence alignments are represented by a " − ".

Downloaded At: 18:41 14 January 2011

Restraints File

The restraints file containing an additional disulfide linkage between $C399_{D2}$ and $C401_{D2}$ that did not correspond to a disulfade linkage in the rhodopsin crystal structure was added as a constraint. Further constraints were added in construction of the model with dopamine bound in the active site these were obtained from a previous D_2 modelling paper by Teeter *et al.* [15]. The *m*-hydroxy and nitrogen of dopamine were constrained to be within hydrogen bonding distance of $Sl97_{D2}$ and $D114_{D2}$, respectively.

Analysing the pdb Files from Modeller

The resultant pdb files from modeller were altered to fix.

- The chain breaks between METI40 and LEU141; ARG145 and TYR146; GLY173 and LEU174; ILE184 and ALA185; ILE297 and HIS298.
- The disulfide linkages between CYS107 and CYS182; CYS299 and CYS301.
- The atoms to be modified were MET1.Nam to MET1.N2; ARG231.Nam to ARG231.N2.

The D_2 receptor is now complete, except where the 100 residues were removed from between helices 5 and 6, although before starting the final minimisation process the joins and disulfide linkages needed minimising. This was necessary as in some cases the connecting bond between corresponding atoms was around 4 Å.Of the different sequential methods of minimisation employed, no great difference was encountered. From here, the final minimisation process took place.

Analysing the Unbound Receptor State

The three resulting pdb files without the agonist dopamine were compared to one another.

TABLE III RMS fit (Å^2) for all atoms are shown in *italics*, the RMS fit (Å^2) for Cα carbons are shown in normal text

RMS fit	*Structure* 1	*Structure* 2	*Structure* 3
Structure 1	0	1.7391	1.2777
Structure 2	*2.8765*	0	1.7131
Structure 3	*2.5587*	*2.7720*	0

Downloaded At: 18:41 14 January 2011

The RMS fit, see Table III, shows that structures 1 and 3 are in closer agreement with one another, especially when just looking at the Cα carbon alignment. The major difference with structure 2 is in the cytoplasmic loop C2 where residues 142 to 144, loop downwards away from the receptor contrary to both other models. The alignment using all atoms indicates that the structures do differ, although from visual analysis this is due to the outside residues of the model where more steric freedom is available. Residues around the proposed binding site, where there is less freedom of movement, show a remarkable similarity to one another.

The table of calculated energies, see Table IV, shows that structures 1 and 3 are noticeably lower in energy than structure 2. This would be due to structure 2 having a different conformation of cytoplasmic loop C2 or due to other areas being in constrained conformations.

The three constructed models all show very similar statistics, see Table V, for the phi and psi region plots; however, the residues implicated in the disallowed regions differ significantly.

Structure 3 seems to be the most reliable model because it was one of the two lower energy structures and the residues implicated in the disallowed regions, from the phi/psi plots, were further from the proposed binding site of dopamine D_2, although all structures were used for comparison to the models of the receptor with dopamine bound.

The water accessible residues [14,18–24], see Fig. 2, shows that these are located on the inside of the helices, with the exception being residues PHE189 to PHE198 on helix 5. Although these residues on TM5 are thought to be water accessible due to an unravelling of this section of the helix [19]. TRP160 located at the bottom of the forth helix also appears to be on the outside (not seen here) of the helix and therefore should not be accessible by water, although SCAM data [24] indicates otherwise. Computational analyses, whereby the TRP160 is substituted for CYS160, have been conducted and do in fact show that the substituted CYS160 is water accessible, but it is just the large size and hydrophobic nature of the TRP160 that excludes it from the inside of the receptor.

TABLE IV Calculated Energies (kcal/mol) of the three unbound structures using differing force fields and Kollman charges

Force field charges	*Kollman all atom Kollman*	*Tripos Kollman*
Structure 1	−5302.618	461.824
Structure 2	−5068.643	641.646
Structure 3	−5363.356	518.543

Downloaded At: 18:41 14 January 2011

TABLE V Procheck phi and psi region plot statistics of residues of the three constructed D_2 structures and the rhodopsin structure these were based upon

	Percent in most favoured regions	*Percent in additional allowed regions*	*Percent in generously allowed regions*	*Percent in disallowed regions*
Structure 1	74.4	20.2	2.5	2.8
Structure 2	75.4	19.2	3.5	1.9
Structure 3	74.8	19.9	2.5	2.8
Rhodopsin	77.7	20.3	1.7	0.3
Rhodopsin*	78.5	18.8	2.3	0.3

*This structure of rhodopsin is the structure that was built to create the threader database file from, see "Construction of the Threader Database file" section.

Downloaded At: 18:41 14 January 2011

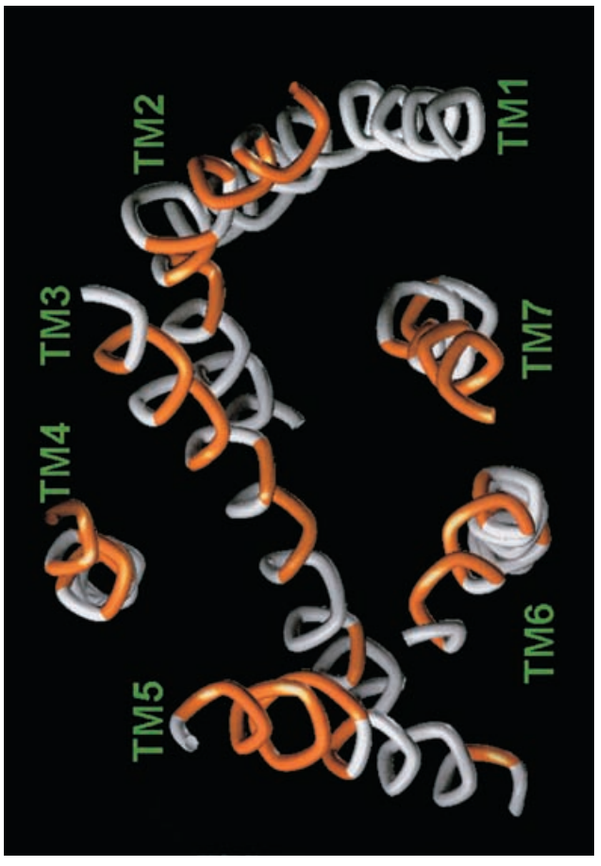

FIGURE 2 Water accessible residues implicated by SCAM.

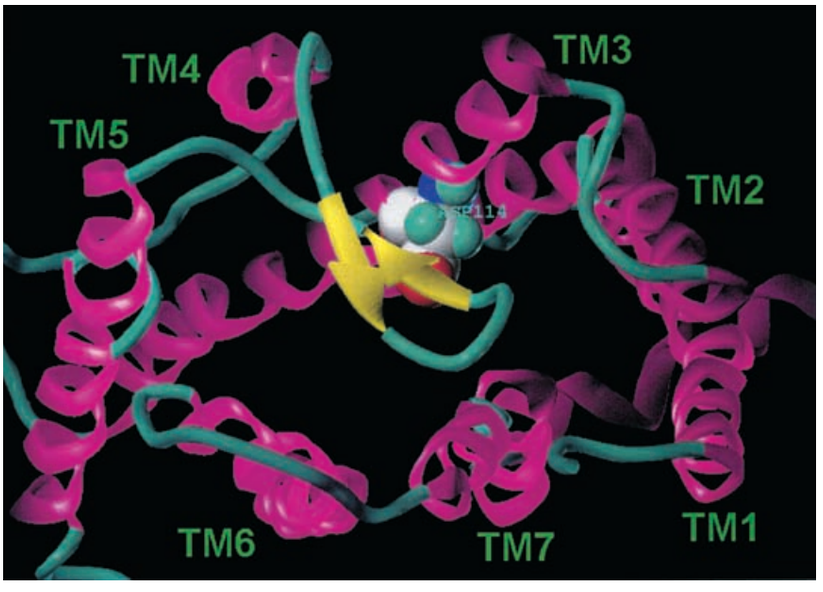

FIGURE 3 Display of secondary structure and ASP114 of unbound structure 3 using Kabasch Sander secondary structure prediction criterion.

The model produced with secondary structure assigned, see Fig. 3, shows the beta sheets present in extracellular loop E2 of the rhodopsin model are also present in the model constructed. This loop also goes deep into the helices and is within six angstrom of the aspartate residue 114 that is implicated in binding compounds, which is consistent with mutagenesis studies that implicate this loop in close proximity to the binding site [24].

Helices 2, 6 and 7 show kinks, see Fig. 3, located around proline residues (not evident in Fig. 3) which is consistent with previous modelling studies. These kinks force the top half of their helices to bend into the plane of the page in a clockwise fashion. Helices 3 and 5 are also entirely tilted into the plane of the page in a clockwise fashion.

TABLE VI RMS fit (Å^2) for all atoms are shown in *italics*, the RMS fit (Å^2) for Cα carbons are shown in normal font

RMS fit	*Structure* 1	*Structure* 2	*Structure* 3
Structure 1	0	1.3084	1.3421
Structure 2	*2.6544*	0	1.3219
Structure 3	*2.6783*	*2.7486*	0

Downloaded At: 18:41 14 January 2011

Downloaded At: 18:41 14 January 2011

Analysing the Bound Receptor State

The three resulting pdb files with the agonist dopamine bound were compared to one another.

The RMS fit statistics, see Table VI, shows that all structures are relatively similar to one another when looking at both the Cα carbon and all atom alignment. Again the residues on the outside of the model, where there are less steric constraints from other residues, differ the greatest and residues around the proposed binding site, where there is less freedom of movement, show a remarkable similarity to one another.

The table of calculated energies, Table VII, shows that structure 1 is the lowest in energy, although structure 2 is of comparable energy. Structure 3 is over 100 kcal/mol higher in energy and thus may not be in the same local minima as the other two structures in different areas of the receptor. The difference in energy between all three structures is less for the bound receptors compared to the unbound receptors, indicating they are better representations of the receptors.

The Procheck phi and psi region plot statistics, see Table VIII, indicates structures 2 and 3 both show comparable statistics; however, structure 1 has twice as many residues in disallowed phi/psi regions. Again the residues implicated in the disallowed regions differ significantly. The structure with most disallowed residues in close proximity to the binding site was surprisingly structure 2, in which ILE184, LEU174 and CYS399 were all in disallowed regions and are all within a radius of less than eight angstrom of dopamine.

Orientation of Dopamine within the Binding Site

In the three models constructed there were two differing conformations of dopamine within the binding site, see Fig. 4. In the two lower energy models, 1 and 2, the aromatic ring of dopamine was almost perpendicular to the axis of the helices, whereas in model 3, the aromatic ring was parallel to the axis of the helices. In all three models hydrogen bonding was seen to take place between the endogenous ligand dopamine and ASP114, SERl97 and SER193.

TABLE VII Calculated Energies (kcal/mol) of the three bound structures using differing Force Fields and Kollman Charges

Force Field charges	*Kollman all atom Kollman*	*Tripos Kollman*
Structure 1	−5533.816	286.861
Structure 2	−5425.183	334.797
Structure 3	−5350.383	581.022

TABLE VIII Procheck phi and psi region plot statistics of residues of the three constructed D_2 receptors with dopamine bound

	Percent in most favoured regions	*Percent in additional allowed regions*	*Percent in generously allowed regions*	*Percent in disallowed regions*
Structure 1	69.7	22.4	3.8	4.1
Structure 2	74.1	21.5	2.5	1.9
Structure 3	74.4	21.1	2.5	1.9

Downloaded At: 18:41 14 January 2011

Comparing the Bound and Unbound Receptor States

Comparison of the models constructed was of much interest as there are a number of differences between the two groups of models.

In the unbound models, we found that the hydrophobic arms of ILE183 and ILE184, from loop E2, orientated themselves into the hydrophobic binding cavity and hence displaced HIS393 relative to the bound models. When the agonist was present, HIS393 was able to penetrate further into the binding cavity and the hydrogenated nitrogen of its pyrrole ring was able to form a hydrogen bond with the carbonyl oxygen of PHE398.

The most interesting find in the analyses of these structures was the changing of the psi(ψ) angle in residue PHE198 and the effect this had on the axis of the helix 5 in two of the three models with the ligand bound.

In two of the three bound models, structures 1 and 3, the less negative psi angle, see Table IX, enabled the amide nitrogen of PHE198 to form an additional hydrogen bond with the carbonyl oxygen of SER193 and/or SER194. This had an effect of altering the bend in the axis, which resulted in a significant displacement of residues further down along the axis of helix 5, see Fig. 5.

The hypothesis that small changes in residues may result in significant conformational changes across the transmembrane helices, and thus participate in molecular mechanisms underlying transmembrane signalling, has been proposed before [29]. Ballesteros *et al.* have statistically shown that the gauche negative (g $-$) chi angle of serine, threonine and cysteine residues affect their phi and psi angles and thus induce or stabilise bends within their helices by formation of an additional hydrogen bond to the $i-3$ or $i-4$ peptide carbonyl oxygen. Interestingly, a similar process from within the SER197 residue mediates the changing of the phi angle for the adjacent PHE198. In the ligand bound models obtained here the two chi angles, structures 1 and 3, for SER197 were in a gauche positive (g $+$) conformation and chi angle for structure 2 was in a trans (t) arrangement, see Table X.

Downloaded At: 18:41 14 January 2011

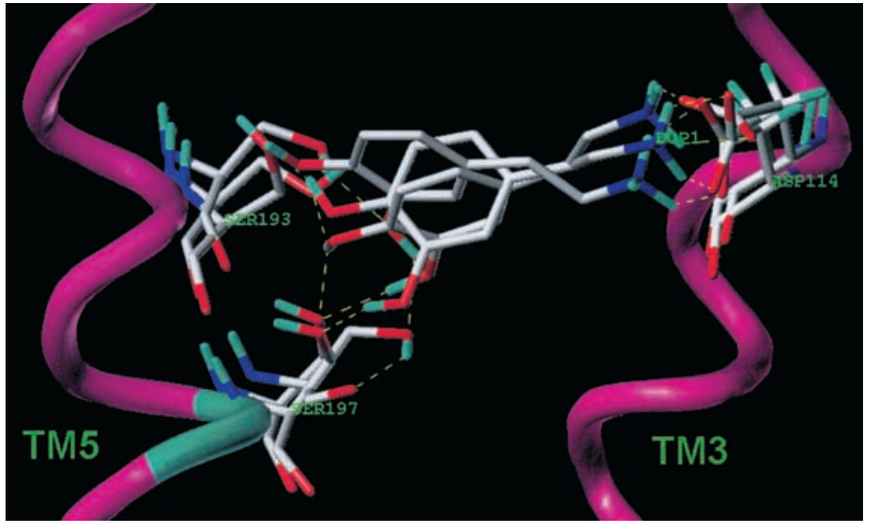

FIGURE 4 Differing conformations of dopamine within the binding site, hydrogen bonding with residues ASP114, SER197 and SER193. Only polar hydrogens are shown.

TABLE IX Psi (Ψ) angle (degrees) for PHE198 in ligand bound and unbound models

	Unbound psi angle	*Bound psi angle*
Structure 1	−141.0	−87.5
Structure 2	−162.3	−167.7
Structure 3	−145.8	−97.7

Downloaded At: 18:41 14 January 2011

TABLE X Phi, psi and chi angles (degrees) for SER197 of ligand bound structures

	phi (ϕ) angle	*psi (Ψ) angle*	*chi (χ) angle*
Structure 1	−82.9	−49.7	82.5
Structure 2	−102.6	26	177.7
Structure 3	−74.9	−42.7	93.3

The two g+ chi angle arrangements have a decreased psi angle and an increased phi angle in SER197, relative to the *t* chi angle arrangement. This effect the chi angle has on the phi/psi angles of SER197 causes the adjoining phi angle of PHE198 to increase and thus be able to form an additional hydrogen bond with SER193 and/or SER194. This in turn leads to a bending of the helix.

In order to test this theory structure 2, with the *t* chi angle, was modified so as to make the chi angle of SER197 g+, and the structure was then initially minimised holding the chi angle rigid then minimised again with no constraints. The resulting structure had a decreased psi angle of SER197 that in turn increased the phi angle of PHE198. This increased phi angle of PHE198 enabled two additional hydrogen bonds to be formed between the amide nitrogen of PHE198 and the carbonyl oxygen of SER194 and SER193 thus altering the bend in the axis of helix 5, see Fig. 6.

This phenomenon of the chi angle of SER197 was only seen when the agonist dopamine was present in the binding site, as two of the unbound models did have g+ chi angles for SER197 and no additional hydrogen bonding between PHE198 and/or SER193/SER194 was seen.

Although a limited number of models were constructed they provide some insights on how the receptor could be activated. These models show the importance of small modifications in residues and the effect this can have on GPCRs, with particular emphasis on SER197 in the D_2 GPCR with dopamine bound.

Downloaded At: 18:41 14 January 2011

FIGURE 5 Cα carbon depiction of helix 5 showing amide nitrogen of PHE198 forming an additional hydrogen bond (dotted line) with the carbonyl oxygen of SER193, compared to the same helix on a different model without this hydrogen bond.

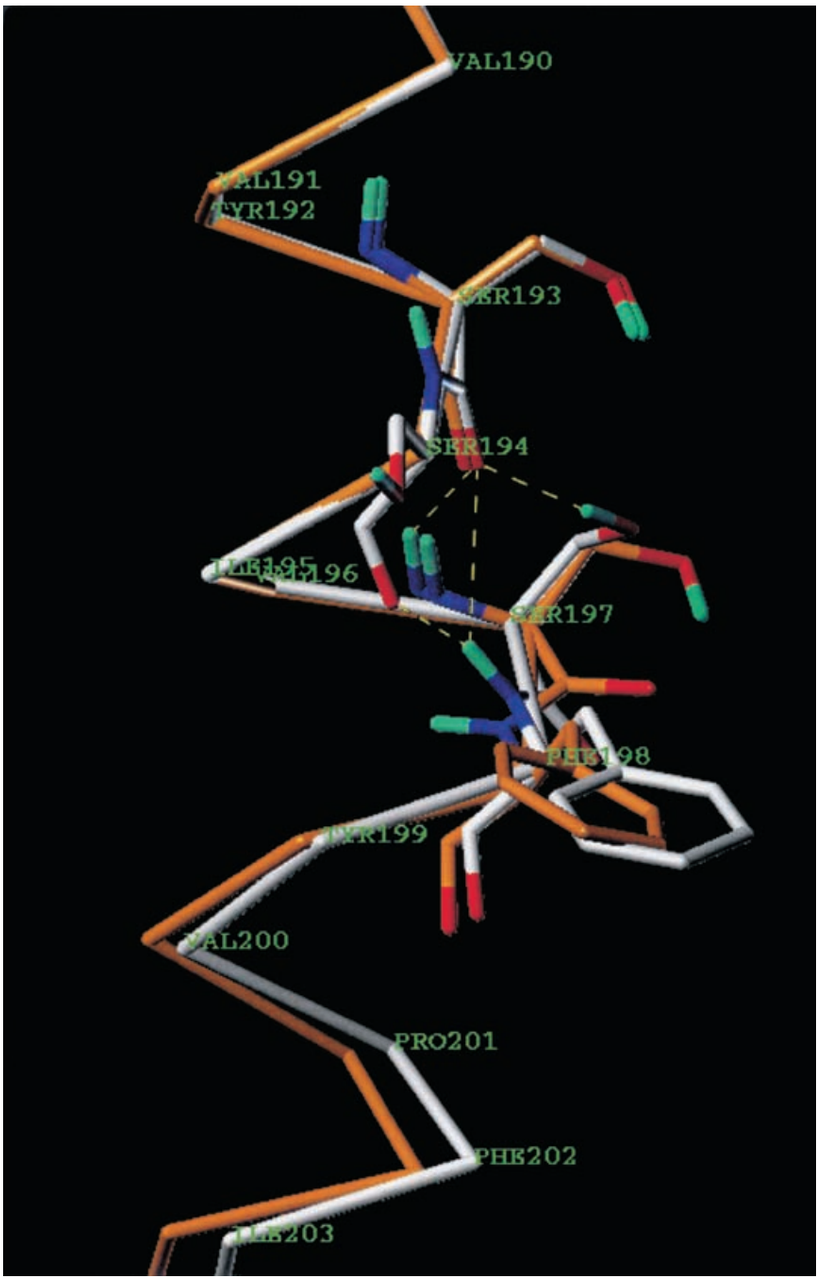

FIGURE 6 Structure 2 after minimisation with the chi angle of SER197 being adjusted from trans to gauche positive compared to the original model of structure 2.

Downloaded At: 18:41 14 January 2011

Downloaded At: 18:41 14 January 2011

CONCLUSION

GPCRs which have important roles in signal transduction at various levels of cellular organisation represent one of the most challenging drug targets for the pharmaceutical industry. In particular, the dopamine D_2 GPCR has been associated with psychosis and the positive symptomatology of schizophrenia.

In order to gain a greater understanding of the D_2 GPCR and the residues involved in the conformational rearrangement within the transmembrane region that may be associated with antipsychotic drug action, we have constructed a number of theoretical models based on the recently published crystal structure of rhodopsin. Until now models have been approximated by the structure of bacteriorhodopsin. As a first step six D_2 receptor models, three with dopamine bound in the active site and three without, were constructed using comparative modelling techniques by alignment of the known D_2 sequence onto rhodopsin. Alignments were analysed and adjusted to account for various factors such as disulfide bonds and highly conserved residues within all GPCRs to give energy minimised three-dimensional D_2 models.

The resulting pdb files having bound dopamine were compared to one another and to the models without dopamine bound. Overall, the RMS fit statistics show that all structures are relatively similar to one another when looking at both the Cα carbon and all atom alignment. Residues on the outside of the model, where there are less steric constraints from other residues, differ the greatest and residues around the proposed binding site, where there is less freedom of movement, show a remarkable similarity to one another.

Of great interest was the orientation of dopamine within the binding site in each of the three models constructed, where two differing conformations of dopamine within the binding site were observed. In the two lower energy models, the aromatic ring of dopamine was almost perpendicular to the axis of the helices, whereas in the remaining model the aromatic ring was parallel to the axis of the helices. In all three models hydrogen bonding was seen to take place between the endogenous ligand dopamine and ASP114, SER197 and SER193.

In the unbound models we found that the hydrophobic arms of ILE183 and ILE184, from loop E2, orientated themselves into the hydrophobic binding cavity and hence displaced HIS393 relative to the bound models. When the agonist was present, HIS393 was able to penetrate further into the binding cavity and the hydrogen bearing nitrogen of its pyrrole ring was able to form a hydrogen bond with the carbonyl oxygen of PHE398. The most interesting finding in the analyses of these structures was the changing of the psi angle in residue PHE198 and the effect this had on the axis of the helix 5 in two of the three models with the ligand bound.

In two of the three bound models, the less negative psi angle, enabled the amide nitrogen of PHE198 to form an additional hydrogen bond with the carbonyl oxygen of SER193 and/or SER194, thus altering the bend in the axis, and resulting in a significant displacement of residues further down along the axis of helix 5. Additionally, this process was only seen to take place when a ligand was present in the binding site. This shows the importance of small modifications in residues and the effect this can have on GPCRs, with particular emphasis on SER197. Whether or not this movement of helix 5 and subsequent additional movement of adjoining helices are the start of the signal transduction process is still under review with various dynamics simulations under way.

Overall this study has shown that robust models of the D_2 GPCR with dopamine bound may be constructed based on rhodopsin by use of comparative modelling techniques and that these models support previously stated mechanistic hypotheses for receptor ligand interactions.

Downloaded At: 18:41 14 January 2011

References

[1] Attwood, T.K. and Findlay, J.B.C. (1994) "Fingerprinting G-protein-coupled receptors", *Protein Engineering* **7**(2), 195.

[2] Wellcome, Glaxo (1996) "Intelligent drug design", *Nature* **384**(Suppl.), 1.

[3] Gudermann, T., Nurnberg, B. and Schultz, G. (1995) "Receptors and G proteins as primary components of transmembrane signal transduction. 1. G-protein-coupled receptors—structure and function [Review]", *Journal of Molecular Medicine* **73**(2), 51.

[4] Seeman, P., Westman, K., Protiva, M., Jilek, J., Jain, P.C., Saxena, A.K., Anand, N., Humber, L. and Philipp, A. (1979) "Neuroleptic receptors: stereoselectivity for neuroleptic enantiomers", *European Journal of Pharmacology* **56**(3), 247.

[5] Palczewski, K., Kumasaka, T., Hori, T., Behnke, C.A., Motoshima, H., Fox, B.A., Le Trong, I., Teller, D.C., Okada, T., Stenkamp, R.E., Yamamoto, M. and Miyano, M. (2000) "Crystal structure of rhodopsin: a G protein-coupled receptor", *Science* **289**(5480), 739.

[6] Berman, H.M., Westbrook, J., Feng, Z., Gilliland, G., Bhat, T.N., Weissig, H., Shindyalov, I.N. and Bourne, P.E. (2000) "The Protein Data Bank", *Nucleic Acids Research* **28**(1): 235-242.

[7] Laskowski, R.A., MacArthur, M.W., Moss, D.S. and Thornton, J.M. (1993) "PROCHECK: a program to check the stereochemical quality of protein structures", *Journal of Applied Crystalography* **26**, 283.

[8] Morris, A.L., MacArthur, M.W., Hutchinson, E.G. and Thornton, J.M. (1992) "Stereochemical quality of protein structure coordinates", *Proteins* **12**, 345.

[9] Hubbard, S.J. and Thornton, J.M. (1993) *NACCESS* (Department of Biochemistry and Molecualr Biology, University College London.

[10] Jones, D.T. (1996) Threader 2 Department of Biological Sciences, University of Warwick.

[10b] Jones, D.T. and Thornton, J.M. (1996) Potential Energy Functions for Threading. *Current Opinion in Structural Biology*. **6**(1): 210-216.

[11] Galtier, N., Gouy, M. and Gautier, C. (1996) "SEAVIEW and PHYLO_WIN: two graphic tools for sequence alignment and molecular phylogeny", *Computer Applications in the Biosciences* **12**(6), 543.

[12] Trumpp-Kallmeyer, S., Hoflack, J., Bruinvels, A. and Hibert, M. (1992) "Modeling of G-protein-coupled receptors: application to dopamine, adrenaline, serotonin, acetylcholine, and mammalian opsin receptors", *Journal of Medicinal Chemistry* **35**(19), 3448.

[13] Sali, A., Sanchez, R. and Badretdinov, A. (1989–1977) Modeller 4 (Rockefeller University, New York).

Downloaded At: 18:41 14 January 2011

[14] Javitch, J.A., Li, X.C., Kaback, J. and Karlin, A. (1994) "A cysteine residue in the third membrane-spanning segment of the human D2 dopamine receptor is exposed in the binding-site crevice", *Proceedings of the National Academy of Sciences of the United States of America* **91**(22), 10355.
[15] Teeter, M.M., Froimowitz, M., Stec, B. and Durand, C.J. (1994) "Homology modeling of the dopamine D-2 receptor and its testing by docking of agonists and tricyclic antagonists", *Journal of Medicinal Chemsitry* **37**(18), 2874.
[16] Tripos, Sybyl. 2000: 1699 South Hanley Road, St Louis, MO 63144, USA.
[17] Weiner, S.J., Kollman, P.A., Nguyen, D.T. and Case, D.A. (1986) "An all atom force field for simulations of proteins and nucleic acids", *Journal of Computational Chemistry* **7**(2), 230.
[18] Javitch, J.A., Fu, D.Y., Chen, J.Y. and Karlin, A. (1995) "Mapping the binding-site crevice of the dopamine D_2 receptor by the substituted-cysteine accessibility method", *Neuron* **14**(4), 825.
[19] Javitch, J.A., Fu, D.Y. and Chen, J.Y. (1995) "Residues in the fifth membrane-spanning segment of the dopamine D_2 receptor exposed in the binding-site crevice", *Biochemistry* **34**(50), 16433.
[20] Fu, D.Y., Ballesteros, J.A., Weinstein, H., Chen, J.Y. and Javitch, J.A. (1996) "Residues in the seventh membrane-spanning segment of the dopamine D2 receptor accessible in the binding-site crevice", *Biochemistry* **35**(35), 11278.
[21] Javitch, J.A., Ballesteros, J.A., Weinstein, H. and Chen, J.Y. (1998) "A cluster of aromatic residues in the sixth membrane-spanning segment of the dopamine D_2 receptor is accessible in the binding-site crevice", *Biochemistry* **37**(4), 998.
[22] Javitch, J.A., Ballesteros, J.A., Chen, J., Chiappa, V. and Simpson, M.M. (1999) "Electrostatic and aromatic microdomains within the binding-site crevice of the D2 receptor: contributions of the second membrane-spanning segment", *Biochemistry* **38**(25), 7961.
[23] Simpson, M.M., Ballesteros, J.A., Chiappa, V., Chen, J., Suehiro, M., Hartman, D.S., Godel, T., Snyder, L.A., Sakmar, T.P. and Javitch, J.A. (1999) "Dopamine D4/D2 receptor selectivity is determined by a divergent aromatic microdomain contained within the second, third, and seventh membrane-spanning segments", *Molecular Pharmacology* **56**(6), 1116.
[24] Javitch, J.A., Shi, L., Simpson, M.M., Chen, J.Y., Chiappa, V., Visiers, I., Weinstein, H. and Ballesteros, J.A. (2000) "The fourth transmembrane segment of the dopamine D_2 receptor: accessibility in the binding-site crevice and position in the transmembrane bundle", *Biochemistry* **39**(40), 12190.
[25] Bairoch, A. and Apweiler, R. (2000) "The SWISS-PROT protein sequence database and its supplement TrEMBL in 2000", *Nucleic Acids Research* **28**(2000), 45.
[26] Sali, A. and Blundell, T.L. (1993) "Comparative protein modelling by satisfaction of spatial restraints", *Journal of Molecular Biology* **234**(3), 779.
[27] Sali, A. and Overington, J. (1994) "Derivation of rules for comparative protein modelling from a database of protein structure alignments", *Protein Science* **3**, 1582.
[28] Luecke, H., Schobert, B., Cartailler, J.P., Richter, H.T., Rosengarth, A., Needleman, R. and Lanyi, J.K. (2000) "Coupling photoisomerization of retinal to directional transport in bacteriorhodopsin [Review]", *Journal of Molecular Biology* **300**(5), 1237.
[29] Ballesteros, J.A., Deupi, X., Olivella, M., Haaksma, E.E.J. and Pardo, L. (2000) "Serine and threonine residues bend alpha-helices in the chi(1) = g(−) conformation", *Biophysical Journal* **79**(5), 2754.